Constructive Interference Steady-State Imaging in Post-Mortem Human Brain: An Alternative or Adjunct to Conventional Autopsy?

J. A. McNab[1], N. Jenkinson[2], T. Aziz[3], and K. L. Miller[1]

[1]Oxford Centre for Functional Magnetic Resonance Imaging of the Brain, University of Oxford, Oxford, United Kingdom, [2]Department of Physiology, Anatomy and Genetics, University of Oxford, United Kingdom, [3]Department of Neurosurgery, University of Oxford, United Kingdom

Introduction Post-mortem diagnosis of neuropathology is an important means of learning more about diseases of the central nervous system and can have a major impact on the management of future patients. In cases where the cause of death is unclear, a conventional autopsy aims to establish a probable cause of death and identify antecedent events leading to death by cutting open the brain and applying a variety of staining methods to tissue samples from suspect brain regions. The costly and time-consuming nature of conventional histological methods usually restricts the examination of the brain to only a few vulnerable regions. Since many types of pathology are localized and difficult to identify on a macroscopic scale, it would be preferable to be able to search for a variety of pathologies in the whole brain. MRI has the benefit of providing whole-brain coverage and does not prevent histology from being carried out post-imaging. Though several studies have previously presented post-mortem MRI[1,2], most have not been optimised for the changed properties of fixed tissue. Due to similar relaxation times in WM and GM conventional T_1, T_2 -weighted imaging protocols no longer provide adequate contrast in fixed tissue. In this study, we present a 3D steady-state imaging protocol, which provides excellent contrast in fixed tissue.

Methods Two whole human brain specimens were scanned on a Siemens 3T Trio system using a 12-channel head coil for signal reception with the appropriate ethics approval for our institution. For imaging the fixed brains were immersed in a proton-free fluid called Fomblin LC/8 (Solvay Solexis Inc.) and secured in a plastic container. Special care was taken to eliminate air-cavities and bubbles within the ventricles and on the surface of the brain. All scanning was performed at room temperature (approximately 23° C). The first brain was from a male 65 year old patient who died of natural causes but had suffered from bipolar disorder and become intractably depressed after experiencing a stroke in his right thalamus. The brain was extracted from the cranium 24 hours post-mortem and soaked in a 10% neutral buffered formalin solution for 6 weeks prior to imaging. Structural images were acquired with a 3D constructive interference steady-state (CISS) pulse sequence using TE/TR = 3.72/7.44 ms, α = 35°, BW = 395 Hz/pixel, matrix size = 576 × 576 × 480, in-plane partial Fourier factor = 5/8, slice partial Fourier factor = 6/8, voxel size = 0.33 × 0.33 mm × 0.33 mm = 0.036 mm^3 and acquisition time per volume = 16 minutes 6 seconds × 32 averages. Quantitative T_1 and T_2 maps were also acquired in this brain using the DESPOT methods[4]. The second brain was from a male patient who had died of natural causes at the age of 66 and did not have any known neuropathology; however, this brain had been fixed for 10 years. For the second brain the resolution of the CISS images was increased to 0.25 × 0.25 mm × 0.25 mm = 0.016 mm^3 with TE/TR = 4.6/9.2 ms, α = 35°, BW = 280 Hz/pixel, matrix size = 688 × 576 × 480, in-plane partial Fourier factor = 5/8, slice partial Fourier factor = 6/8 and acquisition time per volume = 19:54 × 34 averages. In both brains, half of the acquisitions had RF phase = 0° and half had RF phase = 180°. For visualization purposes the contrast of the averaged CISS images has been inverted.

Table 1

Contrast Mechanism	Contrast = S_{GM} - S_{WM}
T_1 - weighted	0.0919
T_2 - weighted	0.1054
CISS	0.1621

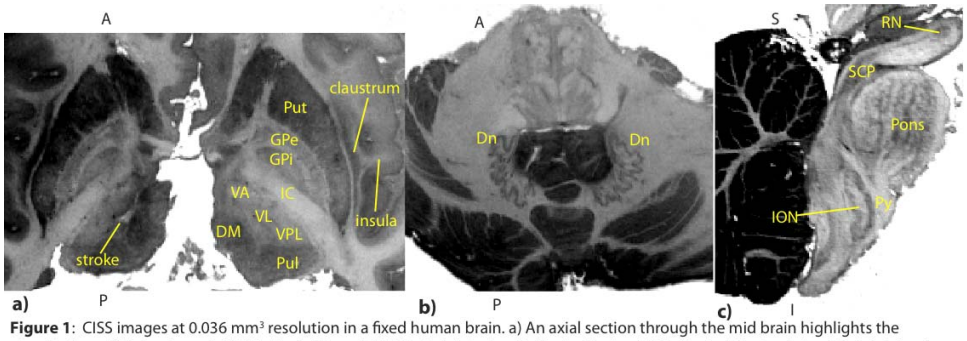

Figure 1: CISS images at 0.036 mm^3 resolution in a fixed human brain. a) An axial section through the mid brain highlights the visualisation of thalamic nuclei (DM: Medial Dorsal, VA: Ventral Anterior, VL: Ventral Lateral, VPL: Ventral Posterolateral, Pul: Pulvinar) as well as clearly defined borders between the internal capsule (IC), globus pallidus internal/externa (GPi/GPe), putamen, claustrum and insula. A right thalamic stroke suffered by this patient 5 years prior to death is clearly visible. b) The dentate nuclei (Dn) are easily identified on an axial section through the cerebellum. c) A sagittal section through the brainstem displays the inferior olivary nucleus (ION), pyramid (Py), pons, superior cerebellar peduncles (SCP) and red nucleus (RN).

Results and Discussion T_1 values in WM and GM in the first specimen were, on average, 340 and 300 ms respectively. T_2 values in WM and GM were 45 and 60 ms respectively. For these relaxation times, Table 1 compares the WM/GM contrast for T_1- /T_2-weighting and CISS. T_1-weighted (1-2**exp*(-TR/T_1)) and T_2-weighted (*exp*(-TE/T_2)) signals were calculated with the TR and TE that maximize WM/GM contrast for the given relaxation times. Since T_1 in WM and GM are so similar there is very little contrast provided by a T_1-weighted protocol, and even T_2–weighting does not provide as much contrast as CISS, which yields signal approximately proportional to T_2/T_1. Figure 1 displays sections of post-mortem CISS images at 0.036 mm^3 resolution. In Figure 1a, the stroke in the right thalamus suffered by this patient appears as a hyperintensity at the border of the medial dorsal and ventral lateral thalamic nuclei. Several other thalamic nuclei and distinct boundaries between the globus pallidus interna/externa are also visible. Even the delicate undulations of the claustrum and surrounding insula can be visualised with ease. In Figure 1b, the highly convoluted, narrow band of neurons that form the dentate nuclei can be seen. Figure 1c also shows several structures not normally visible on *in vivo* MRI such as the inferior olivary nucleus, pyramids, superior cerebellar peduncles and red nucleus. At even higher resolution (0.016 mm^3), images from the second brain specimen (Fig. 2) also excuisite detail including easy identification of thalamic nuclei (Fig. 2a), the inferior cerebellar peduncles, superior vestibular nuclei (Fig. 2b), substania niagra and cerebral penduncles (Fig. 2c).

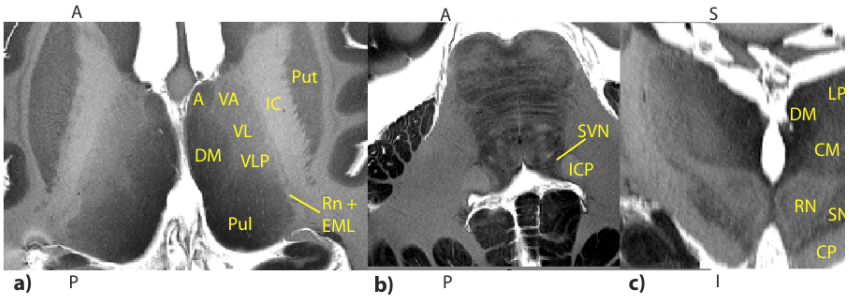

Figure 2: CISS images at 0.016 mm^3 resolution in a fixed human brain. a) An axial section through the mid b highlights the visualisation of thalamic nuclei (A: anterior, DM: medial dorsal, VA: ventral anterior, VL: ventral VPL: ventral posterolateral, Pul: pulvinar, Rn + EML: reticular nucleus and external medullary lamina). Also la are the internal capsule (IC) and putamen (Put). b) An axial section through the pons showing the inferior cerebellar peduncle (ICP) and the superior vestibular nucleus (SVN). c) A coronal section through the mid br showing the cerebral peduncle (CP), substania niagra (SN), red nucleus (RN) and thalamic nuclei DM, VL, LP: l posterior and CM: centromedian).

Conclusion This study presents an MRI protocol for fixed human brain that can be performed on a clinical scanner and provides images at 0.016 - 0.036 mm^3 resolution with exceptional contrast permitting the visualisation of many deep gray matter structures not normally identifiable on *in vivo* images. Historically MRI has lagged behind histological stains for mesostructural detail; however, these images show MRI may be a useful tool for neuropathologists. With the increasing prevalence of 3-Tesla scanners in hospitals, post-mortem imaging is a feasible option for many hospitals and could become a useful adjunct or alternative method for studying diseases of the CNS.

Acknowledgments and References Funding provided by the Charles Wolfson Charitable Trust. The authors would like to thank Dr. Steven Chance for his assistance preparing the specimen for imaging. (1) Amunts K. et. al. NeuroImage 11:66-84 (2000) (2) Eickhoff S. et. al. HBM 24:206-215 (2005). (3) Scheffler K. et. al. Eur Radiol 13:2409-18 (2003). (4) Deoni S.C. et .al. MRM 53:237-241 (2005).